© 2017. Published by The Company of Biologists Ltd | Development (2017) 144, 1107-1112 doi:10.1242/dev.143933

Intestinal epithelial organoids fuse to form self-organizing tubes in floating collagen gels

Norman Sachs[1], Yoshiyuki Tsukamoto[1], Pekka Kujala[2], Peter J. Peters[3] and Hans Clevers[1,*]

ABSTRACT

Multiple recent examples highlight how stem cells can self-organize *in vitro* to establish organoids that closely resemble their *in vivo* counterparts. Single Lgr5$^+$ mouse intestinal stem cells can be cultured under defined conditions forming ever-expanding epithelial organoids that retain cell polarization, cell type diversity and anatomical organization of the *in vivo* epithelium. Although exhibiting a remarkable level of self-organization, the so called 'mini-guts' have a closed cystic structure of microscopic size. Here, we describe a simple protocol to generate macroscopic intestinal tubes from small cystic organoids. Embedding proliferating organoids within a contracting floating collagen gel allows them to align and fuse to generate macroscopic hollow structures ('tubes') that are lined with a simple epithelium containing all major cell types (including functional stem cells) of the small intestine. Cells lining the central contiguous lumen closely resemble the epithelial cells on luminal villi *in vivo*, whereas buds that protrude from the main tube into the surrounding matrix closely resemble crypts. Thus, the remarkable self-organizing properties of Lgr5$^+$ stem cells extend beyond the level of the microscopic cystic organoid to the next, macroscopic, level of tube formation.

KEY WORDS: Organoid, Mini-gut, Matrigel, Collagen gel, Tube, Mouse

INTRODUCTION

The intestinal epithelium is the most rapidly self-renewing tissue of the mammalian body with a turnover time of 4-5 days. The stem cells that drive this self-renewal process reside at the base of the intestinal crypts of Lieberkühn (Clevers, 2013). Several years ago, we developed *in vitro* culture methods allowing the generation and expansion of three-dimensional intestinal organoids from single Lgr5$^+$ adult stem cells (Sato et al., 2009) that we had identified previously (Barker et al., 2007). Essential for epithelial organoid culture are cell embedment within Matrigel and three externally added growth factors that substitute for the absent crypt stem cell niche: (1) epithelial growth factor (EGF); (2) the Wnt agonist and Lgr5 ligand R-spondin; and (3) the BMP inhibitor Noggin. Intestinal organoids contain Lgr5$^+$ adult stem cells that give rise to all differentiated cells at normal ratios (Paneth cells, goblet cells, tuft cells, enteroendocrine cells and enterocytes) and recapitulate central features of the normal gut epithelium, including the organization into crypt and villus domains. When isolated from other normal or diseased tissues, the resulting organoids similarly recapitulate the respective (patho-)physiology (e.g. Boj et al., 2015; Huch et al., 2015; van de Wetering et al., 2015). Organoids expand for years while remaining genetically stable and therefore can be used as experimental, diagnostic and potentially therapeutic tools. Although the advantages and applications of organoids are manifold (Sato and Clevers, 2013a; Clevers, 2016), these cystic structures are merely microscopic mini-versions of the originating epithelial tissue

Larger models of the intestinal epithelium range from air-liquid interface cultures with stroma (Ootani et al., 2009), over cells seeded on biological or synthetic scaffolds (Shaffiey et al., 2016; Torashima et al., 2016) to complex tissue-engineered intestines and living bioreactors (Levin et al., 2013; Grant et al., 2015; Cromeens et al., 2016). Progress in this area has indeed been remarkable, but all cited methods are laborious and technically difficult to perform in laboratories that lack specific tissue-engineering expertise. We therefore sought to develop an easy and fast method to generate macroscopic units of intestinal epithelium that can be performed in any laboratory with tissue culture experience. Here, we describe the self-organization of intestinal organoids into centimeter-long tubes in floating collagen gels.

RESULTS AND DISCUSSION

Organoids self-organize into macroscopic tubes through collagen gel contraction

In vivo, a variety of extracellular matrices provides support for epithelia and significantly influence epithelial and stem cell behavior. It is therefore not surprising that the choice of extracellular matrices in three-dimensional cell culture systems matters a great deal (Gattazzo et al., 2014). For example, we found Matrigel to be indispensable for epithelial organoid culture (Sato et al., 2009), whereas collagen gels have been used for decades, for example, to study fibroblast-mediated wound contraction (Bell et al., 1979). Collagen gels have proven particularly useful because their physical properties can easily be manipulated (e.g. floating versus anchored gels), which in turn greatly influences the phenotypes of embedded cells (Emerman and Pitelka, 1977; Grinnell, 1994). As mammary epithelial cells have been shown to form ducts in collagen gels (Foster et al., 1983), we tested whether mouse small intestinal organoids would be able to similarly organize into macroscopic tube structures. As expected, organoids in conventional plastic-adherent Matrigel droplets overwhelmingly grew as singular budding cysts (Fig. 1A). In sharp contrast, organoids grown in floating collagen gel rings formed a seemingly continuous macroscopic tube within 2 days of plating (Fig. 1B). While buds – crypt analogues – remained present along the tube axis, we noted relatively smooth stretches wherever organoids were seemingly fusing (Fig. 1B). Time-lapse imaging over 24 h revealed that the

[1]Hubrecht Institute, Royal Netherlands Academy of Arts and Sciences (KNAW), and University Medical Center Utrecht, Uppsalalaan 8, Utrecht 3584 CT, The Netherlands. [2]The Netherlands Cancer Institute, Antoni van Leeuwenhoek Hospital, Plesmanlaan 121, Amsterdam 1066 CX, The Netherlands. [3]The Maastricht Multimodal Molecular Imaging Institute, Universiteitssingel 50, Maastricht 6229 ER, The Netherlands.

*Author for correspondence (h.clevers@hubrecht.eu)

N.S., 0000-0002-5467-7151; P.J.P., 0000-0002-2964-5684; H.C., 0000-0002-3077-5582

Received 22 August 2016; Accepted 16 January 2017

Development (2017) 144, 1107-1112 doi:10.1242/dev.143933

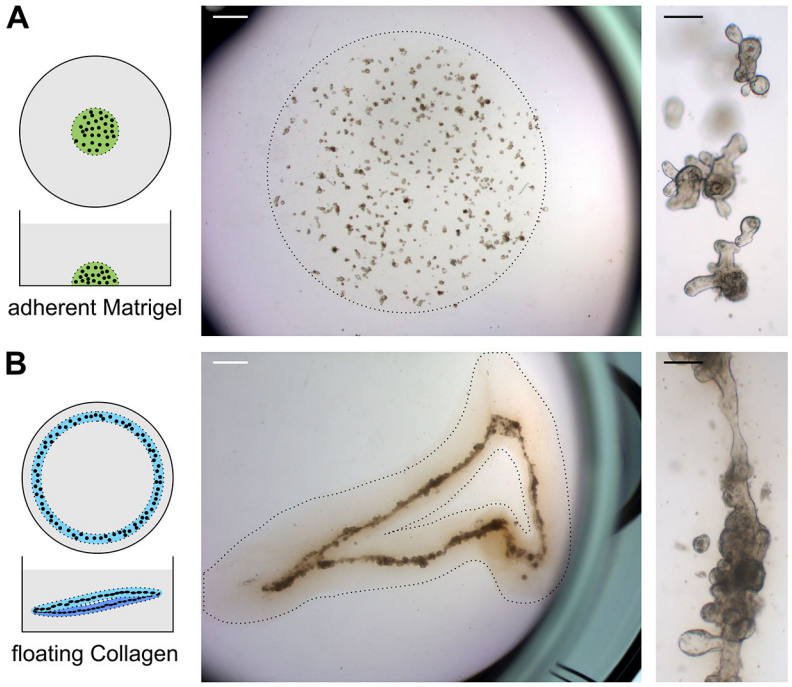

Fig. 1. Organoids in collagen self-organize into tubes. (A) Traditional organoid culture in a plastic-adherent Matrigel drop overlaid with growth medium. Mouse small intestinal organoids mainly grow as single budding cysts. (B) Organoids cultured in floating collagen gel rings form a continuous tube from which buds extend. Both cultures are shown 3 days after plating. Scale bars: 1 mm (middle panel); 100 µm (right panel). Representative images of at least three independent experiments are shown.

floating collagen gels contract over time (Fig. 2A, Movie 1), allowing organoids to physically align adjacent to one another. Gel contraction was driven by organoids and was dependent on collagen I: collagen gels contracted only when organoids were embedded within them, whereas gels formed from Matrigel did not contract regardless of organoid presence (Fig. 2B). Consequently, organoids did not align and form tubes in floating Matrigel rings (Fig. 2C). Similarly, tubes did not form in adherent collagen gels due to the absence of gel contraction and of organoid alignment (Fig. 2C). A floating ring structure is therefore necessary, but not sufficient for tube formation. Tube formation was furthermore dependent on preformed organoids, because single cells were not able to generate tubes in floating collagen gels (Fig. 2C). Organoids have previously been shown to fuse when in close proximity (Jabaji et al., 2014). To test for organoid fusion, we allowed tube formation to occur from independent cultures: we seeded organoids containing membrane-targeted tandem dimer Tomato or membrane-targeted green fluorescent protein (GFP) at a ratio of five to one into floating collagen gels and visualized the resulting tubes using immunofluorescence. We found that green organoids integrated randomly into overwhelmingly red tubes in both budding and smooth domains, with both epithelia merging seamlessly (Fig. 2D). Tube formation can occur through proliferation and/or coalescence (Wozniak and Keely, 2005). Using time-lapse imaging, we indeed visualized that both mechanisms contribute to organoid fusion (Movie 2). In summary, we propose that organoid fusion is driven by proximity of proliferating organoids, based on two movements: (1) the expansion of single organoids; and (2) the contraction of the collagen ring.

Intestinal tubes contain stem and differentiated cells around a continuous lumen

To characterize intestinal tubes in more detail, we analyzed thin histological sections. As shown in Fig. 3A, intestinal tubes are much bigger than intestinal organoids, but still feature a continuous lumen surrounded by a simple monolayered epithelium (organoids <200 µm×200 µm×200 µm, tubes >100 µm×100 µm×2 mm). Lumina of both tubes and organoids contain shed apoptotic cells that arose from intestinal cell turnover. We knew this turnover of terminally differentiated cells in organoids was fueled by proliferating buds (the analogues of *in vivo* crypts) (Sato et al., 2009) and indeed observed the vast majority of $Ki67^+$ cells within crypt domains in both organoids and intestinal tubes (Fig. 3A). The villus domain contained only rare proliferating cells and – as *in vivo* – was composed of enterocytes, goblet cells and enteroendocrine cells, as identified by Hematoxylin and Eosin staining (HE), periodic acid-Schiff stain (PAS) and immunohistochemistry against chromogranin A (Fig. 3B). Proliferating $Ki67^+$ crypt domains were instead composed of alternating slender and large cells (Fig. 3B), indicating the typical pattern of stem and Paneth cells, respectively (Sato et al., 2011). Slender cells indeed occasionally displayed the stem cell-typical high Wnt activity, as identified by nuclear localization of β-catenin (Fig. 3B). The large cells were identified as Paneth cells by PAS staining and lysozyme immunohistochemistry and fluorescence (Fig. 3B). To verify the identity of all cells morphologically, we analyzed intestinal tubes by transmission electron microscopy. As shown in Fig. 3C, crypt domains indeed contained Paneth cells, directly neighboring the typical stem cell, originally described *in vivo* as crypt base columnar cells (Cheng and Leblond, 1974). We furthermore clearly identified mucus-containing goblet cells, secretory vesicle-containing enteroendocrine cells, as well as highly polarized enterocytes with their typical apical brush border (Fig. 3C). We next compared expression of cell type-specific genes in organoid versus tubes. Although the intestinal epithelial marker villin (*Vil1*) was expressed at similar levels, the stem cell marker *Lgr5* and the Paneth cell marker lysozyme (*Lyz1*) were expressed at lower levels in tubes compared with organoids (Fig. 3D). By contrast, markers for enterocytes (*Alpi*) as well as entero-endocrine cells (*Chga*) were expressed at significantly higher levels in tubes (Fig. 3D). Together, these data indicate a larger villus:crypt ratio in tubes compared with organoids. As switching 3D cultures from Matrigel to collagen can induce mesenchymal genes and phenotypes (Nguyen-Ngoc

Development (2017) 144, 1107-1112 doi:10.1242/dev.143933

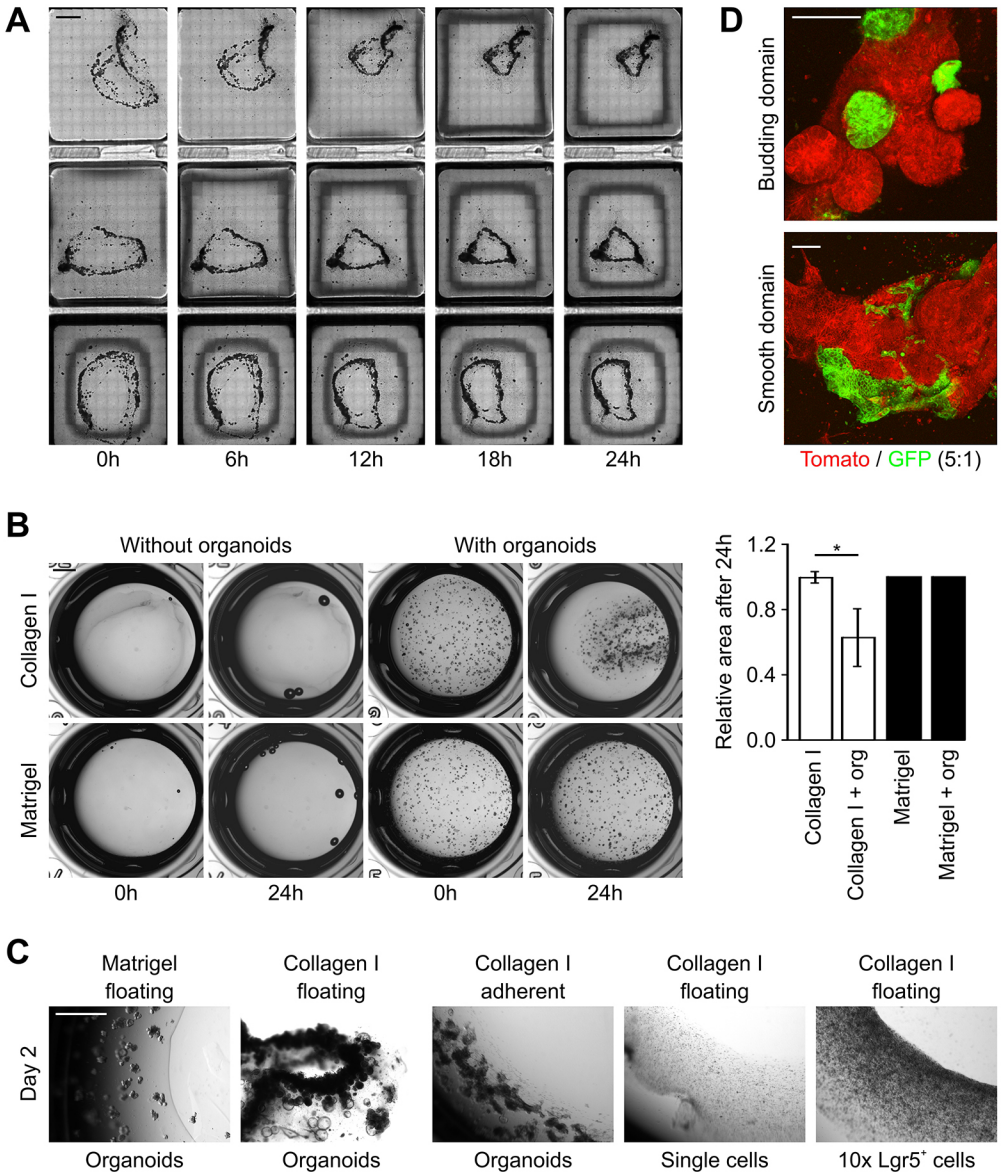

Fig. 2. Tube formation requires gel contraction and organoid fusion. (A) Still images from Movie 1 show collagen gels contracting over time, forcing organoids into alignment and proximity. (B) Bright-field images of gel contraction assays at 0 h and 24 h post-seeding, as indicated. Graph shows quantification of the area taken up by the organoids. Representative images of at least three independent experiments are shown. This physical alignment is noticeably absent in adherent collagen I or floating Matrigel. Organoids induce contraction of collagen, but not of Matrigel. (C) Bright-field images of alternative strategies used to generate tubes. Tube formation requires gel constriction and organoid alignment, which only floating collagen gels provide. Neither floating Matrigel nor adherent collagen gels support tube formation when the same number of organoids are embedded. Single cells do not form tubes (single cells: heterogeneous cell mixture from dissociated organoids grown in regular medium, 10× Lgr5$^+$ cells; Lgr5$^+$ stem cells are from dissociated organoids pre-treated with CHIR99021 and valproic acid seeded at 10×). (D) Tubes formed from two distinctly labeled organoid cultures seeded at a ratio of five to one (red, membrane-targeted tandem dimer Tomato; green, membrane-targeted GFP). Evidently, tubes arise from organoid fusion in both budding (top) and smooth (bottom) domains 3 days after plating. Scale bars: 2 mm in A; 1 mm in B,C; 100 µm in D. (C) Representative examples of at least two independent experiments are shown. (D) Representative examples of three independent experiments are shown.

et al., 2015; Vellinga et al., 2016), we tested expression levels of *Twist1*, *Twist2*, *Zeb2* and vimentin (*Vim*) in collagen-grown tubes compared with Matrigel-grown organoids. They were indeed upregulated (Fig. 3D). However, we did not observe mesenchymal phenotypes (Fig. 3A,B) and as *Twist1* expression also increases along the crypt-villus axis *in vivo* (Mariadason et al., 2005), the increased expression of mesenchymal genes in tubes is likely due to the increased villus:crypt ratio.

To test whether collagen supports regular organoid culture, we embedded freshly isolated mouse small intestinal crypts in adherent collagen gels. Although organoids initially formed, they did not expand and were lost upon passaging (Fig. 4A). Likewise, tubes could only be maintained in collagen gels. However, when we transferred tubes from collagen into Matrigel, small cystic organoids arose from crypt domains within days (Fig. 4B). During a second passage into Matrigel, these organoids were released from the 'remains' of the tube, leaving empty crypt holes and the static villus domain behind (Fig. 4B). Occasionally, organoids formed from the rims of crypt holes, in agreement with *in vivo* findings by us and others: committed progenitor cells can revert to a stem cell phenotype upon depletion of the initial stem cell compartment (Tian et al., 2011; van Es et al., 2012; Tetteh et al., 2016). However, we have never seen *in vitro* or *in vivo* evidence for fully differentiated cells (enterocytes, goblet cells, or Paneth cells) to revert to a stem cell state or to initiate organoids.

Macroscopic intestinal tubes can be used as an *in vitro* model of intestinal epithelium where a larger overall size and/or a bigger villus compartment is beneficial, allowing the investigation of drug effects and gene roles on the structure and development of the intestinal epithelium. Tubes currently do not lend themselves to expansion. Our methods could potentially be applied to organoids from other tissues (normal, diseased and/or genetically modified). Tubes could eventually be employed for regenerative medicine purposes in not only the gut, but – when derived from the pertinent organoids – also in structures such as the trachea and upper airways or in ducts such as the ureter, bile duct or urethra. In conclusion, we have developed a simple and straightforward protocol to generate macroscopic intestinal tubes from small cystic organoids. By embedding organoids within a contracting floating collagen gel, the organoids are physically aligned and fuse to generate macroscopic

Development (2017) 144, 1107-1112 doi:10.1242/dev.143933

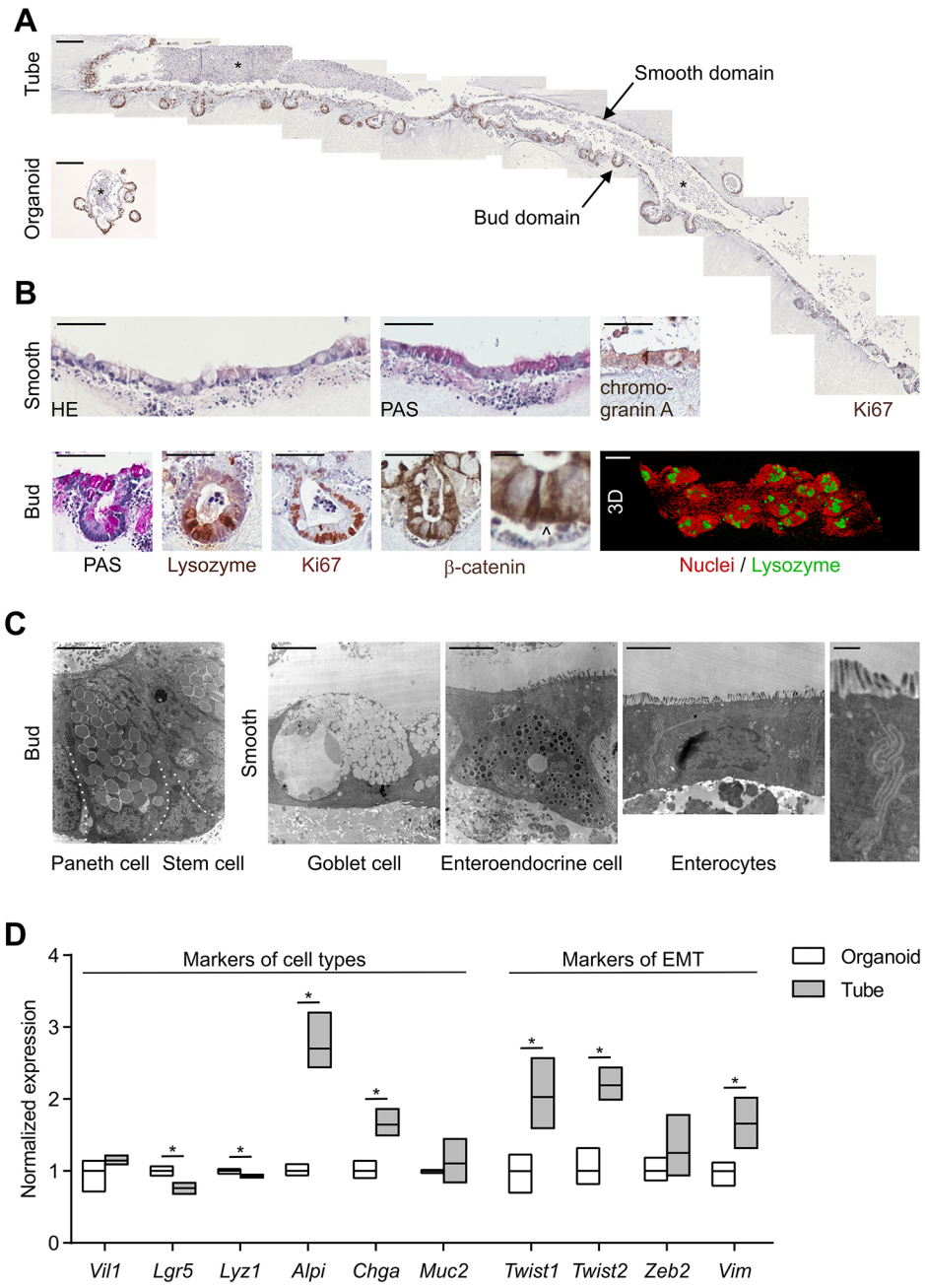

Fig. 3. Tubes contain stem and differentiated cells around a continuous lumen. (A) Composite immunohistochemistry image of a single tube with multiple proliferating buds (Ki67 staining) and a continuous lumen several times the diameter of that of a conventional organoid grown in Matrigel (*). Shed apoptotic cells are present in the lumina of both tube and organoid, owing to intestinal cell turnover. Cultures are shown 4 days after plating. (B) Immunohistochemistry and 3D reconstructed confocal microscopy show details of tube domains. Tubes contain long stretches of simple epithelium (villus domains) with enterocytes (HE), goblet cells (HE, PAS) and enteroendocrine cells (chromogranin A). Buds are crypt-like domains that contain proliferative cells (Ki67) and alternating slender and large cells (β-catenin). Slender cells occasionally display high Wnt activity (nuclear β-catenin, ^), whereas large cells are Paneth cells (PAS, lysozyme). Cultures are shown 4 days after plating. (C) Transmission electron microscopy confirms the presence of Paneth cells that neighbor slender crypt base columnar cells (stem cells) in crypt domains, goblet cells, enteroendocrine cells and enterocytes in villus domains. (D) qPCR analysis of cell type and epithelial-to-mesenchymal transition (EMT) markers using RNA isolated from 4-day-old organoids and tubes. *Vil1* (intestinal epithelium), *Lgr5* (stem cells), *Lyz1* (Paneth cells), *Alpi* (enterocytes), *Chga* (entero-endocrine cells), *Muc2* (goblet cells), and *Twist1*, *Twist2*, *Zeb2* and *Vim* (all mesenchymal markers). Levels of stem cells markers are decreased in tubes, whereas villus and mesenchymal marker levels are increased. *P<0.05 (Student's *t*-test). Scale bars: 100 µm in A; 50 µm in B; 5 µm in C; 1 µm in C (right-most image). (D) Data are pooled from two or three independent experiments.

hollow structures that are lined by a simple epithelium containing all major cell types (including functional stem cells) of the small intestine. The remarkable self-organizing properties of Lgr5$^+$ stem cells do not stop at the level of the microscopic cystic organoid, but extend to the next, macroscopic, level of tube formation.

MATERIALS AND METHODS

Organoid and tube culture

Mouse organoid culture in plastic-adherent Matrigel drops was performed as described previously (Sato and Clevers, 2013b). The establishment of organoid culture from mouse small intestines was approved by the responsible ethical committee (DEC) in compliance with local animal welfare laws, guidelines and policies. For organoid culture in floating collagen rings, 3-day-old organoids were released from Matrigel using cold advanced DMEM/F12 medium and washed three times to remove Matrigel remnants. Collagen gels were prepared by combining cold rat tail collagen I (Invitrogen, final 0.75 mg/ml) with cold ultrapure water (EMD Millipore), cold 10× DMEM/F-12 (Invitrogen) and HEPES (Sigma, final 10 mM). pH was adjusted to 7.4 with sodium hydroxide (Sigma) using pH indicator strips (Merck). Organoids were combined with cold pre-mixed collagen gel at ∼6000 organoids/ml and seeded in a continuous gel ring at the edges of BSA (Life Technologies, 1% w/v in PBS) blocked wells in 24-well suspension plates (Greiner) at ∼1200 organoids in 200 µl/well. Gel rings were solidified at 37°C and subsequently detached by forceful addition of 500 µl organoid culture medium [advanced DMEM/F12 supplemented with penicillin/streptomycin, 10 mM HEPES, Glutamax, B27 (all from Invitrogen), 1 µM N-acetylcysteine (Sigma), 50 ng/ml EGF (BioSource), ∼100 ng/ml Noggin, and 1 µg/ml R-spondin (both R&D Systems)]. Tubes formed within days of seeding. Red- and green-labeled organoids stem from a global double-fluorescent Cre reporter mouse (Muzumdar et al., 2007) before and after Cre-mediated recombination *in vitro*. Passaging of tubes out of collagen gels into Matrigel was achieved by brief incubation with collagenase (Sigma, 1 mg/ml) before washing, mechanical shearing using flamed glass Pasteur pipettes and transfer into 200 µl Matrigel. Lgr5$^+$ stem cells were enriched by pre-treating small intestinal organoids with 3 µM

Development (2017) 144, 1107-1112 doi:10.1242/dev.143933

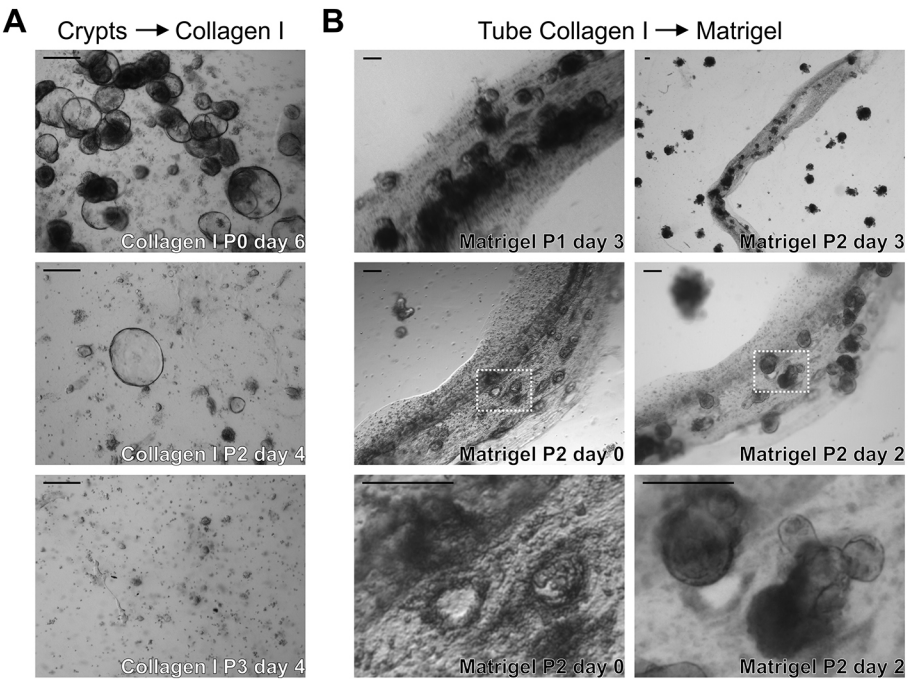

Fig. 4. Tube crypts give rise to organoids. (A) Mouse small intestinal crypts form organoids in adherent collagen gels, but cannot be expanded upon passaging. (B) Transferring tubes from collagen into Matrigel allows crypt domains to form organoids while villus domains remain static. Upon a second Matrigel passage, organoids are released from crypt domains, which stay behind as empty holes. Scale bars: 100 µm. Representative images of at least two independent experiments are shown.

CHIR99021 (Stemgent) and 2 mM valproic acid (Sigma) for 7 days as described previously (Yin et al., 2014). For gel contraction assays, 250 µl of collagen gels or matrigels were added to each well of a 24-well culture plate with or without organoids. After the gels were solidified at 37°C for 30 min, lateral surfaces of the gels were detached from the plate by scraping with pipette tips. The area of each gel was measured by ImageJ immediately after and 24 h after seeding. Data are expressed as the relative area after 24 h compared with the initial area.

Light microscopic analysis, immunofluorescence, histology and immunohistochemistry

Bright-field images of organoid and tube cultures were obtained on Olympus SZX9 and Leica DM IL light microscopes equipped with Leica DFC420C cameras. Time-lapse bright-field imaging was performed on a Leica AF7000 fluorescence microscope equipped with a Leica DFC420C camera after tubes were transferred into eight-well µ-slides (Ibidi). Fluorescent analysis of red and green tubes was performed on a Leica SP5 confocal microscope after tubes were fixed in 4% paraformaldehyde, washed with PBS and mounted in VECTASHIELD hard-set anti-fade mounting medium (Vectorlabs). The same microscope was used to analyze VECTASHIELD whole-mounted tubes after fixation in 4% paraformaldehyde, permeabilization in 0.2% Triton X-100 (Sigma), blocking in 1% BSA, incubation with rabbit anti-lysozyme antibody (DAKO, 1:1000), incubation with anti-rabbit Alexa-568-conjugated antibody (Life technologies, 1:1000) and incubation with DAPI (Life Technologies).

For histological and immunohistochemical analysis, organoids and tubes were fixed in 4% paraformaldehyde, paraffin wax embedded and sectioned for HE, PAS and immunostaining. Primary antibodies for used were mouse anti-Ki67 (MONX10283, Monosan, 1:250), rabbit anti-β-catenin (610154, BD transduction, 1:1000), rabbit anti-lysozyme (A0099, DAKO, 1:1000) and goat anti-chromogranin A (sc-1488, Santa Cruz, 1:100). The secondary antibodies were the respective peroxidase-conjugated antibodies for mouse (K4001, DAKO), rabbit (DPVR110HRP, Immunologic IL) and goat (6160-01, Southern Biotech; DPVR110HRP, Immunologic IL) primary antibodies. Histological images were acquired on a Leica Eclipse E600 microscope equipped with a Leica DFC500 camera.

Electron microscopic analysis

Tubes in collagen gels were fixed in Karnovsky's fixative (2% paraformaldehyde, 2.5% glutaraldehyde, 0.1 M sodium cacodylate, 2.5 mM $CaCl_2$ and 5 mM $MgCl_2$ at pH7.4) for 6 h at room temperature. The samples were embedded in Epon resin and were examined with a Phillips CM10microscope.

Quantitative RT-PCR

To determine the expression levels of selected genes, organoids and tubes were cultured in Matrigel drops and floating collagen rings, respectively, for 4 days. Their total RNA was extracted using a RNeasy mini kit (Qiagen) and subjected to qRT-PCR analysis using GoScript Reverse Transcriptase (Promega) and Power SYBR Green PCR Master Mix (Applied Biosystems), in accordance with the manufacturers' instructions. All assays were normalized by the Hprt internal control. The primers used were as follows: villin 1 (forward 5′-ATGACTCCAGCTGCCTTCTCT-3′, reverse 5′-GCTCTGGGTTAGAGCTGTAAG-3′), Lgr5 (forward 5′- ACCCGCC-AGTCTCCTACATC-3′, reverse 5′- GCATCTAGGCGCAGGGATTG-3′), lysozyme (forward 5′-GGAATGGATGGCTACCGTGG-3′, reverse 5′-C-ATGCCACCCATGCTCGAAT-3′), Alpi (forward 5′-AGGATCCATCT-GTCCTTTGG-3′, reverse 5′-ACGTTGTATGTCTTGGACAG-3′), chro-mogranin A (forward 5′-CTCGTCCACTCTTTCCGCAC-3′, reverse 5′-CTGGGTTTGGACAGCGAGTC-3′), Muc2 (forward 5′-ATGCCCACC-TCCTCAAAGAC-3′, reverse 5′-GTAGTTTCCGTTGGAACAGTGAA-3′), Twist1 (forward 5′-CGGAGACCTAGATGTCATTGTTT-3′, reverse 5′-CGCCCTGATTCTTGTGAATTTG-3′), Twist2 (forward 5′-GCCAG-GTACATAGACTTCCTC-3′, reverse 5′-TCATCTTATTGTCCATCTCG-TC-3′), Zeb2 (forward 5′-GATTTCAGGGAGACTTGCTG-3′, reverse 5′-ACAGACAGGAATCGGAGTC-3′) and vimentin (forward 5′-GAGGAG-ATGCTCCAGAGAGA-3′, reverse 5′-TCCTGCAAGGATTCCACTTT-3′).

Acknowledgements

We are grateful to Jeroen Korving and Harry Begthel for the preparation of histological and immunohistochemical specimens. We also thank Anko de Graaff and the Hubrecht Imaging Center for supporting the imaging.

Competing interests

H.C. is an inventor on several patents involving the organoid culture system. All other authors declare no competing interests.

Author contributions

N.S. designed, performed and analyzed experiments, and wrote the manuscript. Y.T. designed, performed and analyzed experiments, and commented on the manuscript. P.K. and P.P. performed electron microscopy and commented on the manuscript. H.C. supervised the study and wrote the manuscript.

Funding
This work was supported by the Nederlandse Organisatie voor Wetenschappelijk Onderzoek (NWO/VENI 916.15.182 to N.S.), the Grant-in-Aid for Scientific Research International (Japan Society for the Promotion of Science, 15KK0351 to Y.T.) and the Netherlands Organization for Health Research and Development (ZonMW/TAS 40-41400-98-1108 to H.C.).

Supplementary information
Supplementary information available online at
http://dev.biologists.org/lookup/doi/10.1242/dev.143933.supplemental

References

Barker, N., van Es, J. H., Kuipers, J., Kujala, P., van den Born, M., Cozijnsen, M., Haegebarth, A., Korving, J., Begthel, H., Peters, P. J. et al. (2007). Identification of stem cells in small intestine and colon by marker gene Lgr5. *Nature* **449**, 1003-1007.

Bell, E., Ivarsson, B. and Merrill, C. (1979). Production of a tissue-like structure by contraction of collagen lattices by human fibroblasts of different proliferative potential in vitro. *Proc. Natl. Acad. Sci. USA* **76**, 1274-1278.

Boj, S. F., Hwang, C.-I., Baker, L. A., Chio, I. I. C., Engle, D. D., Corbo, V., Jager, M., Ponz-Sarvise, M., Tiriac, H., Spector, M. S. et al. (2015). Organoid models of human and mouse ductal pancreatic cancer. *Cell* **160**, 324-338.

Cheng, H. and Leblond, C. P. (1974). Origin, differentiation and renewal of the four main epithelial cell types in the mouse small intestine. V. Unitarian Theory of the origin of the four epithelial cell types. *Am. J. Anat.* **141**, 537-561.

Clevers, H. (2013). The intestinal crypt, a prototype stem cell compartment. *Cell* **154**, 274-284.

Clevers, H. (2016). Modeling development and disease with organoids. *Cell* **165**, 1586-1597.

Cromeens, B. P., Liu, Y., Stathopoulos, J., Wang, Y., Johnson, J. and Besner, G. E. (2016). Production of tissue-engineered intestine from expanded enteroids. *J. Surg. Res.* **204**, 164-175.

Emerman, J. T. and Pitelka, D. R. (1977). Maintenance and induction of morphological differentiation in dissociated mammary epithelium on floating collagen membranes. *In Vitro* **13**, 316-328.

Foster, C. S., Smith, C. A., Dinsdale, E. A., Monaghan, P. and Neville, A. M. (1983). Human mammary gland morphogenesis in vitro: the growth and differentiation of normal breast epithelium in collagen gel cultures defined by electron microscopy, monoclonal antibodies, and autoradiography. *Dev. Biol.* **96**, 197-216.

Gattazzo, F., Urciuolo, A. and Bonaldo, P. (2014). Extracellular matrix: a dynamic microenvironment for stem cell niche. *Biochim. Biophys. Acta* **1840**, 2506-2519.

Grant, C. N., Mojica, S. G., Sala, F. G., Hill, J. R., Levin, D. E., Speer, A. L., Barthel, E. R., Shimada, H., Zachos, N. C. and Grikscheit, T. C. (2015). Human and mouse tissue-engineered small intestine both demonstrate digestive and absorptive function. *Am. J. Physiol. Gastrointest. Liver Physiol.* **308**, G664-G677.

Grinnell, F. (1994). Fibroblasts, myofibroblasts, and wound contraction. *J. Cell Biol.* **124**, 401-404.

Huch, M., Gehart, H., van Boxtel, R., Hamer, K., Blokzijl, F., Verstegen, M. M. A., Ellis, E., van Wenum, M., Fuchs, S. A., de Ligt, J. et al. (2015). Long-term culture of genome-stable bipotent stem cells from adult human liver. *Cell* **160**, 299-312.

Jabaji, Z., Brinkley, G. J., Khalil, H. A., Sears, C. M., Lei, N. Y., Lewis, M., Stelzner, M., Martin, M. G. and Dunn, J. C. Y. (2014). Type I collagen as an extracellular matrix for the in vitro growth of human small intestinal epithelium. *PLoS ONE* **9**, e107814.

Levin, D. E., Sala, F. G., Barthel, E. R., Speer, A. L., Hou, X., Torashima, Y. and Grikscheit, T. C. (2013). A "living bioreactor" for the production of tissue-engineered small intestine. *Methods Mol. Biol.* **1001**, 299-309.

Mariadason, J. M., Nicholas, C., L'Italien, K. E., Zhuang, M., Smartt, H. J. M., Heerdt, B. G., Yang, W., Corner, G. A., Wilson, A. J., Klampfer, L. et al. (2005). Gene expression profiling of intestinal epithelial cell maturation along the crypt-villus axis. *Gastroenterology* **128**, 1081-1088.

Muzumdar, M. D., Tasic, B., Miyamichi, K., Li, L. and Luo, L. (2007). A global double-fluorescent Cre reporter mouse. *Genesis* **45**, 593-605.

Nguyen-Ngoc, K.-V., Shamir, E. R., Huebner, R. J., Beck, J. N., Cheung, K. J. and Ewald, A. J. (2015). 3D culture assays of murine mammary branching morphogenesis and epithelial invasion. *Methods Mol. Biol.* **1189**, 135-162.

Ootani, A., Li, X., Sangiorgi, E., Ho, Q. T., Ueno, H., Toda, S., Sugihara, H., Fujimoto, K., Weissman, I. L., Capecchi, M. R. et al. (2009). Sustained in vitro intestinal epithelial culture within a Wnt-dependent stem cell niche. *Nat. Med.* **15**, 701-706.

Sato, T. and Clevers, H. (2013a). Growing self-organizing mini-guts from a single intestinal stem cell: mechanism and applications. *Science* **340**, 1190-1194.

Sato, T. and Clevers, H. (2013b). Primary mouse small intestinal epithelial cell cultures. *Methods Mol. Biol.* **945**, 319-328.

Sato, T., Vries, R. G., Snippert, H. J., van de Wetering, M., Barker, N., Stange, D. E., van Es, J. H., Abo, A., Kujala, P., Peters, P. J. et al. (2009). Single Lgr5 stem cells build crypt-villus structures in vitro without a mesenchymal niche. *Nature* **459**, 262-265.

Sato, T., van Es, J. H., Snippert, H. J., Stange, D. E., Vries, R. G., van den Born, M., Barker, N., Shroyer, N. F., van de Wetering, M. and Clevers, H. (2011). Paneth cells constitute the niche for Lgr5 stem cells in intestinal crypts. *Nature* **469**, 415-418.

Shaffiey, S. A., Jia, H., Keane, T., Costello, C., Wasserman, D., Quidgley, M., Dziki, J., Badylak, S., Sodhi, C. P., March, J. C. et al. (2016). Intestinal stem cell growth and differentiation on a tubular scaffold with evaluation in small and large animals. *Regen. Med.* **11**, 45-61.

Tetteh, P. W., Basak, O., Farin, H. F., Wiebrands, K., Kretzschmar, K., Begthel, H., van den Born, M., Korving, J., de Sauvage, F., van Es, J. H. et al. (2016). Replacement of lost Lgr5-positive stem cells through plasticity of their enterocyte-lineage daughters. *Cell Stem Cell* **18**, 203-213.

Tian, H., Biehs, B., Warming, S., Leong, K. G., Rangell, L., Klein, O. D. and de Sauvage, F. J. (2011). A reserve stem cell population in small intestine renders Lgr5-positive cells dispensable. *Nature* **478**, 255-259.

Torashima, Y., Levin, D. E., Barthel, E. R., Speer, A. L., Sala, F. G., Hou, X. and Grikscheit, T. C. (2016). Fgf10 overexpression enhances the formation of tissue-engineered small intestine. *J. Tissue Eng. Regen. Med.* **10**, 132-139.

van de Wetering, M., Francies, H. E., Francis, J. M., Bounova, G., Iorio, F., Pronk, A., van Houdt, W., van Gorp, J., Taylor-Weiner, A., Kester, L. et al. (2015). Prospective derivation of a living organoid biobank of colorectal cancer patients. *Cell* **161**, 933-945.

van Es, J. H., Sato, T., van de Wetering, M., Lyubimova, A., Nee, A. N., Gregorieff, A., Sasaki, N., Zeinstra, L., van den Born, M., Korving, J. et al. (2012). Dll1+ secretory progenitor cells revert to stem cells upon crypt damage. *Nat. Cell Biol.* **14**, 1099-1104.

Vellinga, T. T., den Uil, S., Rinkes, I. H. B., Marvin, D., Ponsioen, B., Alvarez-Varela, A., Fatrai, S., Scheele, C., Zwijnenburg, D. A., Snippert, H. et al. (2016). Collagen-rich stroma in aggressive colon tumors induces mesenchymal gene expression and tumor cell invasion. *Oncogene* **35**, 5263-5271.

Wozniak, M. A. and Keely, P. J. (2005). Use of three-dimensional collagen gels to study mechanotransduction in T47D breast epithelial cells. *Biol. Proced. Online* **7**, 144-161.

Yin, X., Farin, H. F., van Es, J. H., Clevers, H., Langer, R. and Karp, J. M. (2014). Niche-independent high-purity cultures of Lgr5+ intestinal stem cells and their progeny. *Nat. Methods* **11**, 106-112.